FAR-INFRARED PROPERTIES OF METALLIC MESH AND ITS COMPLEMENTARY STRUCTURE

R. ULRICH*

Physikalisches Institut der Universität, 78 Freiburg, Hermann-Herder-Str. 3, Germany

Abstract—The optical properties of thin metallic mesh ("inductive" grids) are compared theoretically and experimentally with the properties of the complementary structure ("capacitive" grids). Close interrelations are found. In the non-diffraction region (wavelength > grid constant), the optical properties of both types of grids can be described by simple transmission line equivalent circuits. The circuit parameters are determined as functions of the dimensions of the grids. This representation allows a fairly accurate calculation of interference filters consisting of two or more grids of either type. The new capacitive grids may be used advantageously in interference filters with non-harmonic lying orders, in filters with strongly differing peak transmissions, and in effective low-pass filters in the very far-infrared.

1. INTRODUCTION

METALLIC mesh is used in far-infrared optics as filter,[1, 2] as beam splitter,[3] and as reflector in interference filters.[4] This paper reports recent measurements of the transmission and reflection of the usual metallic mesh; but primarily it is concerned with the optical properties of the structure which is complementary to metallic mesh: this new structure consists of thin square disks of metal, arranged in a plane, regular, pattern of square symmetry [Fig. 1(b)]. The disks are supported by a thin transparent film. A grid of this type will be called a "capacitive" grid, in contrast to the usual metallic mesh [Fig. 1(a)], which will be referred to as an "inductive" grid.

The following treatment will be restricted to thin grids ($t \ll a$) of either type. Therefore, its conclusions are valid only for the electroformed metallic mesh† and for the thin capacitive grids (their preparation is described in the Appendix). The results need not necessarily be applicable to metallic mesh woven of wires of circular cross-section,[2] for which $t > a$. For both capacitive and inductive grids simple relations connect transmissivity, reflectivity, and the corresponding phases, and therefore a measurement of one of these is sufficient to determine the other optical properties. The comparison of two complementary grids shows that their transmissivities etc. are complementary, also. These theoretical relations between the various optical properties are proved by measurements at a selected number of grids. From these measurements also a general, empirical, description of the optical properties of thin grids as a function of their dimensions is obtained. It is advantageous to use for this purpose the representation by an electrical transmission line equivalent circuit. A simple oscillatory circuit is found sufficient to represent the properties of the grids with considerable accuracy over nearly the whole non-diffraction region $\lambda > g$. This equivalent circuit

---

* Now at: National Physical Laboratory, New Delhi 12, India.
† Buckbee Mears Co., St. Paul, Minn. U.S.A. Sumitomo Shoji Kaisha Ltd., Osaka, Japan, Prof. Heimann, Wiesbaden-Dotzheim, Germany.
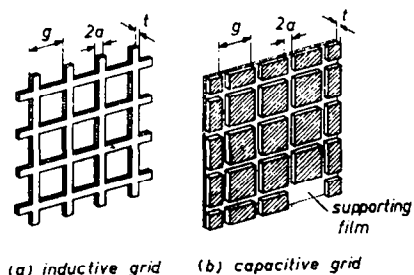
FIG. 1. The inductive and the capacitive two-dimensional grid.

representation is applied to the calculation of interference filters consisting of either capacitive grids solely or combined with inductive ones. The full advantage of this representation will appear, however, only in the calculation of multi-grid filters. Such filters with effective low-pass characteristics will be treated in a separate paper.

2. THEORETICAL COMPARISON OF CAPACITIVE AND INDUCTIVE GRIDS

2.1 General Properties

Three idealizations are made: the grids are assumed to be infinitely thin, the metallic parts of the grids are considered as perfectly conducting, and the influence of the dielectric film, supporting the capacitive grid, is neglected. The admissibility and the consequences of these idealizations will be discussed later.

A plane, electromagnetic wave of unit amplitude may be incident normally on a grid of either type. The surface currents in the grid produce a scattered field in which the electrical field is distributed symmetrically and the magnetic field asymmetrically to the plane of the grid.[5] If the wavelength is $\lambda > g$, the only propagating parts of the scattered field are the zero order transmitted and the zero order reflected waves. Their equal (electrical) amplitudes are described by the complex reflection coefficient Γ. From a simple dimensional analysis it is clear that Γ depends on the grid constant g and on the wavelength λ only through the ratio $\omega = g/\lambda$ which will be called henceforth "normalized" frequency. Diffraction is absent in the region $\omega < 1$. "Behind" the grid the originally incident wave and the scattered wave Γ superpose and constitute the transmitted wave. Its amplitude τ is given by the fundamental relation

$$\tau(\omega) = 1 + \Gamma(\omega) \tag{1}$$

Since the losses are neglected, simultaneously with (1)

$$|\tau(\omega)|^2 + |\Gamma(\omega)|^2 = 1 \tag{2}$$

must hold. As a consequence, the phases $\psi_\tau(\omega)$ and $\psi_\Gamma(\omega)$ of the transmission and reflection coefficients, respectively, are related directly to the power transmissivity $|\tau(\omega)|^2$ which can be measured most easily among all optical properties of a grid:

$$\sin^2 \psi_\tau(\omega) = |\tau(\omega)|^2 \tag{3a}$$

$$\sin^2 \psi_\tau(\omega) = 1 - |\tau(\omega)|^2 \tag{3b}$$

The locus of $\Gamma(\omega)$ in the complex plane, following by elimination of τ from (1) and (2), is the circle drawn in Fig. 2. With varying frequency the points of the vectors Γ and τ move along this circle. At all frequencies the reflected and the transmitted wave are seen to be 90° out of phase. Under the mentioned idealizations these considerations apply to either type of grid in the range $\omega < 1$.
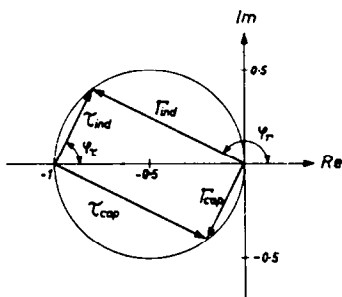

FIG. 2. The locus of the amplitude reflection (Γ) and transmission (τ) coefficients of a thin, lossless, capacitive, grid and of the complementary inductive grid in the complex plane. Valid if $g/\lambda < 1$. The phases of Γ and τ are indicated for the inductive grid; they should read ψ_Γ and ψ_τ.

2.2 Complementary Grids

The comparison of complementary grids is possible using the electromagnetic equivalent of Babinet's principle. In its general form[6] it relates the electromagnetic diffraction fields around a thin, perfectly conducting, perforated, screen with the fields around the complementary screen; the plane of polarisation of the incident wave must be, however, in the second case perpendicular to that in the first case. Now, for a two-dimensional grid with square symmetry and a normally incident wave, the zero order transmission and reflection coefficients are independent of the direction of polarisation. This can be verified easily by decomposing the incident wave into two parts which oscillate parallel to the two main symmetry-directions of the grid. Both parts are transmitted (reflected) in the same way. Then they add to a transmitted (reflected) wave of the same polarisation as the incident wave. As τ and Γ show this independence of polarisation, the application of Babinet's principle to an inductive grid and its complementary capacitive grid yields

$$\tau_i(\omega) + \tau_c(\omega) = 1 \qquad (4)$$

or with respect to (1):

$$\tau_i(\omega) = -\Gamma_c(\omega) \qquad \text{and} \qquad \tau_c(\omega) = -\Gamma_i(\omega) \qquad (5)$$

The subscripts i and c refer to the inductive and capacitive grid, respectively. The relations (5) are illustrated in Fig. 2. From (2) and (5) the interesting fact follows that not only the amplitude transmissivities are complementary (4), but also the power transmissivities:

$$|\tau_i(\omega)|^2 + |\tau_c(\omega)|^2 = 1 \qquad (6)$$

The equations (4–6) are the desired interrelations for complementary grids.

Nothing can be learned from these general considerations about the special form of

either $|\tau_i(\omega)|^2$ or $|\tau_c(\omega)|^2$. Their calculation would require the solution of Maxwell's equations with the appropriate boundary conditions in the plane of the grid. However, from the fact that infinitely extended d.c. currents are possible in the inductive grid, it can be concluded directly that for $\omega \to 0$ the inductive grid must reflect like a metallic mirror, i.e. $\Gamma_i(0) = -1$, whereas the capacitive grid must become completely transparent: $\Gamma_c(0) = 0$.

2.3 Absorption

Up to now the absorption of the grids has been neglected. Practically it may result from the ohmic losses of the surface currents flowing in the metallic parts of the grids, and, in a capacitive grid, also from dielectric losses in the supporting film. The ohmic losses will be estimated now and it will be shown that their neglection is admissible in most cases for grids of good conducting metals: for an incident wave of unit amplitude the average change of magnetic field-strength across the grid is 2Γ. This is caused by an average surface current density $\bar{J} = c\Gamma/4\pi$ (in cgs units) on either side of the grid. If the skin depth δ ($\delta = 0.12\,\mu$ in copper at $\lambda = 1$ mm) is small compared with the thickness t of the grid, the real part of the surface impedance is $\rho = 1/\delta\sigma$, where $\sigma = $ conductivity. The dissipated power per unit area of the grid becomes $P_d = 2\rho J_{\text{eff}}^2 = 2\rho\,\eta\,J^{-2}$. Here a dimensionless form-factor η has been introduced to take account of the difference between the spatial r.m.s. value J_{eff} and the above calculated average value $\bar{J}$ of the current. This difference is due to the non-uniform spatial distribution of the current in the plane of the grid. As a rough estimation, $1/\eta$ can be equalled to that relative part of the cross-section of the grid which may conduct current: $\eta = 1/(1 - 2a/g)$ for the capacitive grid, and $\eta = g/2a$ for the inductive one. Now a comparison of P_d with the power density $P_o = c/4\pi$ of the incident wave yields the absorptivity $A = P_d/P_o$ of a grid due to ohmic losses:

$$A = |\Gamma|^2\,\eta\,(c/\lambda\sigma)^{1/2} \tag{7}$$

Using the bulk d.c.-conductivity of copper and $\lambda = 0.5$ mm, one has $(c/\lambda\sigma)^{\frac{1}{2}} = 10^{-3}$. Even if a considerable degradation of the surface conductivity due to a microscopic roughness of the metallic surface is allowed for,[6] the absorptivity (7) is fairly low in the far infrared region. It is in the order of 10^{-3} for capacitive grids and, because of η, perhaps 10^{-2} for inductive ones.

The dielectric losses in the substrate of the capacitive grid are higher than they would be in the same substrate without a grid, since the electrical field energy is concentrated in the gaps between the metallic pieces. A simplified estimation shows that they are higher by the factor $g/2a$. Choosing a sufficiently thin substrate of a low-loss material, the dielectric losses can be kept as low as the ohmic losses or lower. Simultaneously the refractive influence of the substrate decreases. In the following measurements the optical thickness of the substrate was in the order of $\lambda/100$ and less, and never was any influence of the substrate observed.

3. MEASUREMENTS OF CAPACITIVE AND INDUCTIVE GRIDS

The aim of the measurements was to determine the unknown functions $|\tau(\omega)|^2$ for capacitive grids, and to check whether the relations (3) and (6), which were derived under idealized assumptions, hold for real grids of finite thickness and finite conductivity.

Several capacitive grids have been prepared by a photo-etching technique from copper

layers on Mylar (see Appendix). They are listed in Table 1 along with three commercial inductive grids. The far infrared properties of these grids were investigated with a periodic working Fourier-spectrometer[7] equipped with a low-temperature receiver for the 5–35 cm^{-1} frequency range. All measurements were performed at normal incidence with a beam semi-aperture of 7°. For reasons discussed above unpolarized radiation could be used.

TABLE 1. DIMENSIONS OF THE MEASURED GRIDS

	Grid		Dimension (μ)				Equivalent circuit parameters		
No.	Type	Material	g	a	t	a/g	Z_0	ω_0	R
1	Cap.	Cu on Mylar	368	17·7	5	0·051	0·274	1·0	<0·02
2	Ind.	Ni*	368	17·0	14	0.046	3·00	1·0‡	0·02†
3	Cap.	Cu on Mylar	250	40·5	5	0·161	0·70	0·96	<0·02
4	Cap.	Cu on Mylar	473	72·5	5	0·153	0·73	0·96	0·001†
5	Cap.	Cu on Mylar	342	68·5	6	0·200	1·19	0·945	0·002†
6	Ind.	Cu*	216	28·8	7	0·133	1·33	1‡	0·004†
7	Ind.	Ni*	216	13·5	12	0·0625	2·42	1‡	<0·04
8	Cap.	Cu on Mylar	368	(35)§	7	(0·095)	(0·48)§	1‡	—

The equivalent circuit parameters refer to the equivalent circuits of Table 3. They are determined by adoption of the calculated $|\tau|^2$ to the measurements.
 * Product of Buckbee Mears Co., St. Paul, Minn. U.S.A.
 † Ohmic losses only, calculated from (15) for $\lambda = 0.5$ mm and $\sigma = 0.25\ \sigma_{bulk}$
 ‡ Chosen arbitrarily.
 § See Appendix.

3.1 Transmissivity

In Fig. 3 the transmissivities of the grids are shown as a function of the normalized frequency $\omega = g/\lambda$. In this way grids with different grating constants can best be compared. The behaviour of the capacitive grids obviously is complementary to that of the
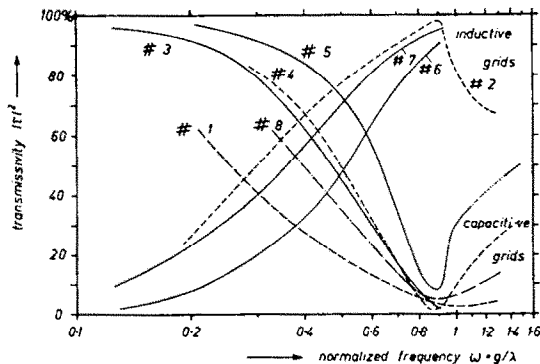

FIG. 3. Measured transmissivities of capacitive and inductive grids. The dimensions of the grids are given in Table 1.

inductive grids: the inductive grid acts as a high-pass in the region $\omega < 1$, whereas the capacitive grid has low-pass properties. This is in agreement with equation (6). The steepness of the transmissivity curves depends on the ratio a/g of the grids: capacitive grids with low a/g, i.e. with relatively small gaps between the metallic disks, have a smooth transmission curve, and its minimum is located at $\omega = 1$. For higher a/g, i.e. broader gaps, the cutoff becomes steeper and the minimum shifts slightly toward lower frequencies. For the measured inductive grids, too, the steepness of the transmission curve increases with a/g. The desired proof of the complementarity (6) is tried in Fig. 4. There the sum of the measured power transmissivities of the complementary grids No. 1 and No. 2 is nearly unit throughout a broad frequency region $\omega < 1$. The deviation of the sum from
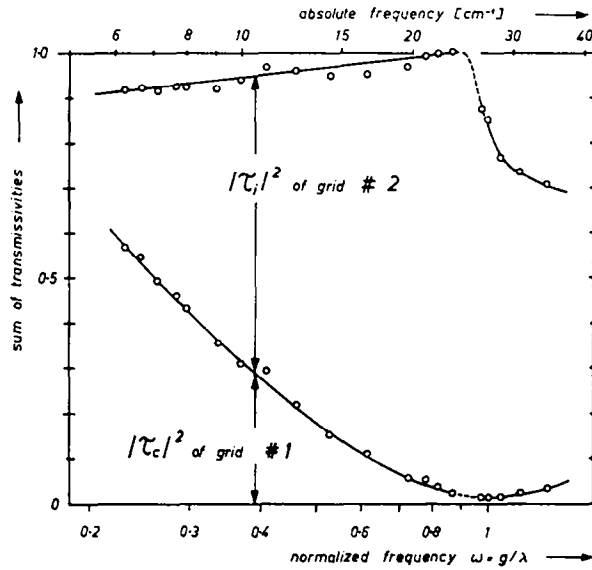

FIG. 4. The sum of the measured power transmissivities of two nearly complementary grids (No. 1 and No. 2 of Table 1).

unit may partially be due to absorption in both grids, but the major part of it is caused probably by the finite thickness of the inductive grid. This finite thickness is considered the reason for other deviations, too, shown by the inductive grid in the phase measurements discussed below and in the comparison with one-dimensional gratings. The deviation in Fig. 4 would be even a little more pronounced if the two grids were truly complementary (see dimension a in Table 1). This could not be achieved, however, with the rather primitive photoetching technique employed.

3.2 Phases

A test of the relations (3) among the transmissivity and the phases required a measurement of the phase $\psi_r(\omega)$ of the reflectivity. For this purpose an interference filter was formed from two identical samples of the grid under investigation. The grids were held plane and parallel to each other at a variable, but known, distance by the support depicted in Fig. 5. The grids were glued to frames and spanned over the faces B and C, respectively. Face A is a reference plane that may be used to place a third and a fourth grid (in a similar

support) parallel to the first ones. The distance between the grids could be adjusted by means of the spring-loaded, calibrated, thread. The faces A, B, and C remained parallel within a few microns if ring 1 was turned with respect to 2.

For the determination of the amplitude reflectivity $\Gamma(\omega)$ the power transmissivity of the interference filter was recorded as a function of the distance of the grids. From the
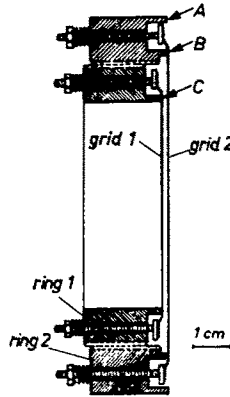

FIG. 5. Cross-section through interference filter. The annular faces A, B, C of the brass rings 1,2, have been commonly ground optically flat in the zero position of the calibrated screw

positions of the observed interference maxima the phase $\psi\Gamma(\omega)$ was evaluated, a multiple of π remaining as an arbitrary additive constant. This was chosen to bring Γ into the negative real half of the complex plane, according to Fig. 2. These phase measurements were done for the capacitive grid No. 3 and the inductive grid No. 7. The results are plotted in Fig. 6. There the indicated points have the distances $(1 - | \ \tau(\omega) \ |^2)^{1/2}$ from
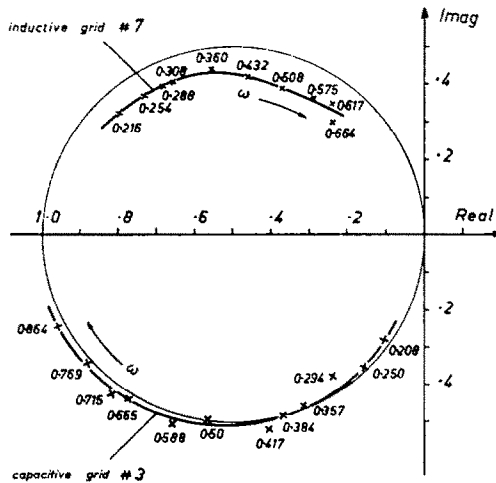

FIG. 6. Measured amplitude reflection coefficients of the capacitive grid No. 3 and the inductive grid No. 7. Parameter on the curves is the normalized frequency $\omega = g/\lambda$. The full circle is expected theoretically for thin lossless grids.

the origin and the arguments $\psi_\Gamma(\omega)$, i.e. they would represent $\Gamma(\omega)$ if the absorption were neglected. The points measured for the capacitive grid lie fairly close to the theoretical circle known from Fig. 2 for thet hin, lossless, grid. Therefore this capacitive grid and the others of similar relative dimensions may well be treated as infinitely thin, and equations (3) are applicable.

The agreement is less satisfying for the inductive grid No. 7. Its points in Fig. 6 show a clear deviation of up to $|\Delta\Gamma| = 0\cdot08$ from the ideal circle. A very similar deviation is found if Russel and Bell's[8] measurements of an inductive grid are plotted in the complex Γ-plane: the points $\tau(\omega) - 1$, calculated from their $\tau(\omega)^2$ and $\psi_\tau(\omega)$, should coincide with the thin-grid-circle. In fact these points lie approximately as far above the circle as the measured points in Fig. 6 lie below it. A first reason for these deviations may be the absorption due to ohmic losses, which were shown to be considerably higher for the inductive grid than for the capacitive one. The absolute influence of absorption should be very small, however, and cannot explain these large deviations. Most probably their reason is that the inductive grids were too thick ($t/g = 0\cdot055$ for the inductive grid No. 7, in contrast to only $t/g = 0\cdot020$ for the capacitive grid No. 3). The influence of the thickness on Γ can be studied approximately by means of the formulae given by Marcuvitz[6] for one-dimensional gratings. It will be shown later that they have close relations to the two-dimensional grids discussed here. These formulae indicate that due to the finite thickness the Γ-curve of an inductive grating is shifted in the negative imaginary direction, and the curve ($\tau(\omega) - 1$) in the opposite direction, both in accordance with the observations. The absolute value of the Γ-shift, calculated for a grating of the same thickness as grid No. 7 is, however, only the third part of the observed deviation. This may be an inherent difference between one-dimensional gratings and two-dimensional grids. The mentioned formulae indicate further that the influence of a given thickness on Γ is much more pronounced for the inductive grid than it is for the capacitive one, or: the value of t/g, up to which a grid acts as a "thin" grid, is lower for the inductive than for the capacitive grid. In view of this, the treatment of the inductive grids of Table 1 as infinitely thin, also, in the following sections is only a rough, but useful, approximation.

It should be mentioned that for the evaluation of the phases generally the second or a higher order interference maximum was used. The corresponding distances of the two grids in the interference filter were sufficiently large to insure that the evanescent, higher order, diffraction sidewaves did not overlap and did not contribute to the interference. Accordingly, no influence of the relative orientation of the symmetry axes of the two grids was observed at $\omega < 1$.

3.3. *Absorption*

The absorptivity A of the capacitive grids of Table 1 was so small that it could not be measured accurately. An upper limit for A followed, however, from the measured peak transmission of the interference filters during the phase measurements: the absorptivity A of the capacitive grid No. 3 does not exceed 2 % in the region $\omega \geqslant 0\cdot5$. A part of this 2 % limit is probably still caused by small imperfections of the grids, by deviations from their ideal parallelism, and by the finite resolution of the spectrometer. At frequencies $\omega > 0\cdot5$ these errors had a rapidly increasing influence, and no experimental determination of A was possible there. The absorptivity of the inductive grid No. 7 is generally higher. The upper limit, determined as above, varies from 1·5 % at $\omega = 0\cdot43$ to 3·3 % at $\omega = 0\cdot21$.

This is in agreement with the estimation (7) if there for σ approximately 1/4 of the d.c.-conductivity of nickel is used. This seems reasonable in view of the influence of surface roughness.

4. EQUIVALENT CIRCUIT REPRESENTATION

The advantage of an equivalent circuit representation of the optical properties of the grids is that it allows the application of the well developed transmission line theory to the calculation of optical filters consisting of two or more grids. This representation becomes especially useful if an equivalent circuit can be chosen which consists of constant (frequency independent) inductances, capacitances, and perhaps ohmic resistors. This representation, and an approximate determination of the circuit parameters as functions of the dimensions of the grids, are the aims of this section.

4.1 *The Susceptance of a Grid*

As the scattered electrical field, produced by a plane wave incident normally on a thin grid, is symmetric to the plane of the grid, the total electrical field is continuous across the grid. The magnetic field, in contrast, has a discontinuity.[5] Therefore, the general equivalent circuit of the thin grid may be a transmission line, representing free space, shunted at the reference plane T by a lumped admittance $2Y$, representing the grid [Fig. 7(a)]. The characteristic admittance of the transmission line is arbitrarily taken as unit,
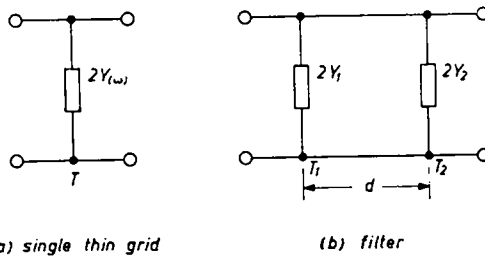

(a) single thin grid   (b) filter

FIG. 7. (a). General equivalent circuit a thin grid in free space. Valid if $g/\lambda < 1$. (b) Equivalent circuit of an interference filter consisting of two grids.

i.e. all other admittances are normalized relative to this one. This representation of the grid in free space by a four-terminal network is possible only at $\omega < 1$ where no propagating diffraction orders exist. The transmission line theory shows that the shunt $2Y$ gives rise to a voltage reflection coefficient

$$\Gamma(\omega) = - Y(\omega)/[1 + Y(\omega)] \tag{8}$$

and to a voltage transmission coefficient

$$\tau(\omega) = 1/[1 + Y(\omega)] \tag{9}$$

These expressions are consistent with (1) and therefore uniquely determine Y, if Γ or τ is known. Thus it is possible to express the optical properties $\tau(\omega)$ and $\Gamma(\omega)$ of any thin grid in the region $\omega < 1$ by the equivalent circuit Fig. 7(a) by an appropriate, frequency dependent, admittance $Y(\omega)$. If the grid is lossless its admittance becomes a pure susceptance

$$Y(\omega) = jB(\omega) \tag{10}$$

with real $B(\omega)$. Then also the equations (3) are satisfied and the locus of Γ in the complex plane is again the full circle of Fig. 2. According to (8) the lower half of this circle belongs to capacitive susceptances $B > 0$, and the upper half to inductive susceptances $B < 0$. Now from the position of the measured values of Γ in the complex plane (Fig. 6) the reason for the notation "capacitive" and "inductive" grids becomes clear: the name of a grid corresponds to the type of susceptance in its equivalent circuit. This is in accordance with Marcuvitz's[6] use of these notations for other microwave–"optical" elements.

The optical properties of two complementary, thin, lossless, grids had been found to be connected by (5). This relation can also be expressed in the equivalent-circuit-picture: The susceptances $B_c(\omega)$ and $B_i(\omega)$ of complementary grids obey

$$B_c(\omega) \cdot B_i(\omega) = -1 \tag{11}$$

4.2 The Equivalent Circuit

For a complete description of the optical properties of the grids now the explicit determination of $B(\omega)$ is necessary. This function contains all informations about $|\tau(\omega)|^2$, $|\Gamma(\omega)|^2$, $\psi_\tau(\omega)$, and $\psi_\tau(\omega)$. Inversely, $B(\omega)$ can be determined from each of these functions. Besides on ω, the susceptance $B(\omega)$ depends also on the dimensions of the given grid, but only through the ratio a/g. For the grids contained in Table 1 the functions $B(\omega)$ can be evaluated from the measured transmissivities (Fig. 3). Thus a good qualitative and quantitative survey of $B(\omega, a/g)$ can be achieved. Here, however, the $B(\omega, a/g)$ will not be given directly, but rather in an indirect way which is more convenient for calculations and which is a consequent application of the concept of the equivalent circuit: an equivalent circuit is synthesized from constant inductances and capacitances to exhibit the susceptance function $B(\omega)$ evaluated from the measurement of $|\tau(\omega)|^2$ of the grids. A grid then is represented by the special network and by the values of its components, i.e. all optical properties are determined by a set of a few numbers rather than by a function $B(\omega)$.

The synthesis of this network is possible under rather general conditions*. Generally the accuracy of the representation depends on the number of components used in the circuit. A first approximation is to use a single element: a fixed capacitance $2C$ for the capacitive grid and, respectively, a fixed inductance $L/2$ for the inductive grid. The optical properties resulting from this simplest circuit are given in Table 2. The numerical values of C and L, respectively, may be adapted so that the calculated $|\tau(\omega)|^2$ fits best the measured transmissivities Fig. 3. In Fig. 8 the calculated $|\tau(\omega)|^2$ is represented by the dashed curve. Its general shape would allow an adaption to the measured $|\tau(\omega)|^2$ only in the low-frequency limit $\omega \to o$. There this simple circuit is useful. At $\omega \to 1$, however, it fails completely. There the measured transmissivity vanishes for the capacitive grid, and it approaches unity for the inductive one. The corresponding susceptances become infinity and zero, respectively. A frequency dependence of this type, but with the same low-frequency behaviour as above, can be realized by adding a second element to the equivalent circuit which completes it as a series or parallel oscillatory circuit, respectively. The resonance of this circuit can be chosen to lie at or near $\omega = 1$ and produces there the necessary pole or zero of $B(\omega)$. The full line in Fig. 8 demonstrates how close an approximation of the measured transmissivity is possible by this 2-element equivalent

---

* $Y(\omega)$ must not have a negative real part which would correspond to negative losses.[9]
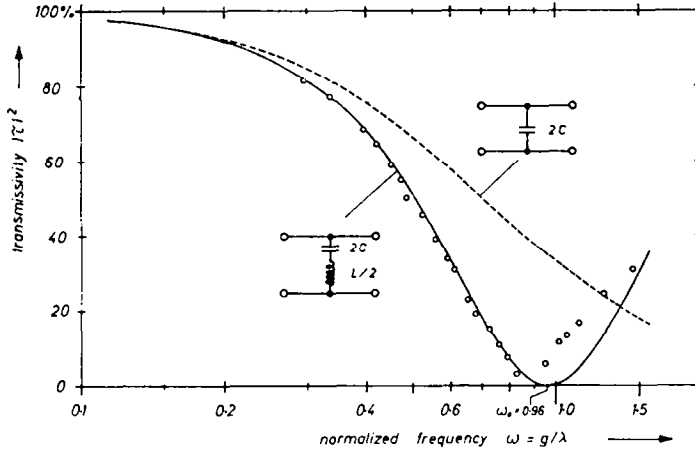
FIG. 8. Approximation of the measured transmissivity of the capacitive grid No. 4 by a 1-element and by a 2-element equivalent circuit. Both circuits have equal capacitances and therefore equal asymptotic behaviour at low frequencies. $2C = 2.85$; $L/2 = 0.318$.

circuit over nearly the whole non-diffraction region $\omega < 1$. From the preceeding general considerations it is sure that simultaneously the other optical properties ($|\Gamma|^2$, ψ_τ, ψ_Γ) are represented correctly, i.e. with comparable accuracy.
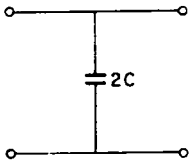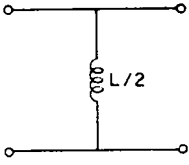
4.3 *The Circuit Parameters*

Two parameters can be adapted to fit a measured transmissivity curve by that calculated from the 2-element equivalent circuit. These parameters are chosen to be the normalized resonant frequency ω_0 and the "characteristic" impedance $Z_0 = \omega_0 L = 1/\omega_0 C$ of L and C at resonance. The main relations valid for this 2-element circuit may be taken from Table 3 if there the loss resistance $R = 0$ is used.

The determination of the characteristic values Z_0 and ω_0 was performed for all grids of Table 1 by fitting their transmissivity curves Fig. 3. For all capacitive grids the fit was possible so that the calculated and the measured curves coincided in two points, at least. Deviations occured only near $\omega = 1$, as is typically illustrated in Fig. 8. For the inductive grids the fit generally was less accurate, and $\omega_0 = 1$ was used in order to get a unique Z_0. These difficulties are considered to be caused again by the finite thickness of the inductive grids. Perfectly "thin" inductive grids should show properties truly complementary to the capacitive grids and should allow an equally accurate fit as these. The relation (11) yields for the characteristic parameters of complementary grids

$$Z_{0i} \cdot Z_{0c} = 1 \quad \text{and} \quad \omega_{0i} = \omega_{0c} \tag{12}$$

The characteristic parameters Z_0 and w_0 of a thin, lossless, grid can only depend on the ratio a/g of the dimensions of the grid. In order to determine these dependences generally, the empirical impedances Z_0 of all grids of Table 1 are plotted in Fig. 9 as a function of this "shape parameter" a/g. There have been measured too few grids, of course, to allow an accurate determination of the general function $Z_0 = Z_0(a/g)$ from these few points. It is important, however, to note that the Z_0-values of the capacitive grids with low a/g coincide remarkably well with the impedance curve $Z_0^{(1)}(a/g)$ which can be calculated from

TABLE 2. SINGLE ELEMENT EQUIVALENT CIRCUITS FOR THIN CAPACITIVE AND INDUCTIVE GRIDS, AND THEIR OPTICAL PROPERTIES. ONLY THE LOW FREQUENCY APPROXIMATIONS ARE IN GOOD AGREEMENT WITH THE MEASUREMENTS

Type of grid:		Capacitive grid	Indutive grid
Equivalent circuit		$\perp$ 2C	L/2
Normalized admittance	$Y(\omega) =$	$j\omega C$	$- j/\omega L$
Reflectivity	$|\Gamma|^2 =$	$\omega^2 C^2/(1 + \omega^2 C^2)$	$1/(1 + \omega^2 L^2)$
	$\psi_\Gamma =$	$\pi + \arctan (1/\omega C)$	$\pi - \arctan \omega L$
Transmissivity	$|\tau|^2 =$	$1/(1 + \omega^2 C^2)$	$\omega^2 L^2/(1 + \omega^2 L^2)$
	$\tau_\tau =$	$- \arctan \omega C$	$\arctan (1/\omega L)$
For complementary grids:		$C_{cap} = L_{ind}$	
Low frequency approximations (valid if $\omega \ll 1$):			
Reflectivity	$|\Gamma|^2 =$	$\omega^2 C^2$	$1 - \omega^2 L^2$
	$\psi_\Gamma =$	$3\pi/2 - \omega C$	$\pi - \omega L$
Transmissivity	$|\tau|^2 =$	$1 - \omega^2 C^2$	$\omega^2 L^2$
	$\psi_\tau =$	$- \omega C$	$\pi/2 - \omega L$

Marcuvitz's[6] theoretical treatment of the *one-dimensional*, thin, capacitive* strip grating:

$$Z_0^{(1)}(a/g) = \frac{1}{2\ln \text{cosec} (a\pi/2g)} \tag{13}$$

The excellent quantitative agreement of the measured impedance Z_0 of 2-dimensional capacitive grids with the impedance (13) calculated for 1-dimensional capacitive gratings in the limit $a/g \to 0$ is not surprising: The 2-dimensional grid differs from the 1-dimen-

---

* A one-dimensional grating is "capacitive" if the electric vector of the incident wave is polarised normally to the lines of the grating. The impedance function (13) was obtained from Marcuvitz,[6] Section 5.1. His equation (2a) was specialized for normal incidence, $g/\lambda \to 0$ and $\omega_0 = 1$.

sional grating only by the additional gaps of width $2a$ in the strips of the grating. As these gaps are oriented parallel to the electrical field and thus to thes urface currents in the strips, their presence or absence has only little influence on the currents, and this influence must completely vanish as $2a \to 0$. Therefore, the function (13) may well be used as the impedance Z_0 of any 2-dimensional capacitive grid of low a/g. For grids of higher a/g $(= 0 \cdot 12 - 0 \cdot 20)$ the impedance Z_0 may be taken approximately from Fig. 9 (dashed
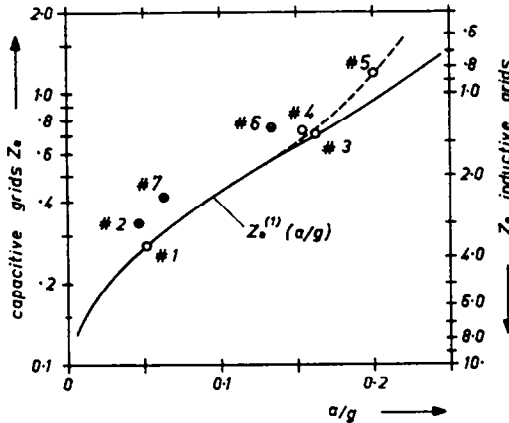

FIG. 9. The characteristic impedances of the grids of Table 1 as a function of the shape-parameter a/g of the grids. ○○ capacitive grids, ⊗⊗ inductive grids. The full line is the theoretical characteristic impedance of one-dimensional gratings in the limit $\omega \ll 1$.

curve). This impedance is higher than the impedance of a 1-dimensional grating, since the transmissivity and consequently the Z_0 of a 1-dimensional grating is increased by the introduction of the broader gaps in the strips. The characteristic impedances Z_0 determined for the *inductive* grids are also represented in Fig. 9, according to (12). They deviate clearly from the curve (13) that was found to be correct for thin, lossless grids. The reasons for these deviations are those discussed already above.

The values ω_0, obtained by fitting the transmissivities of the capacitive grids with various ratios a/g, may be interpolated by

$$\omega_0(a/g) = 1 - 0 \cdot 27 \, (a/g) \tag{14}$$

As the fit was made always with the aim to represent the measured $|\tau(\omega)|^2$ by the calculated expression accurately in a frequency region as broad as possible, the ω_0 from (14) need not be equal (and generally *is* not equal) to the frequency of the measured minimum of the transmissivity (compare Fig. 8). Equation (14) was determined from the adaption of only 4 capacitive grids and should, therefore, not be considered to be absolutely certain. However, as (14) yields ω_0 always close to unit for probably the most interesting region $p/g \leqslant 0 \cdot 2$, the possible errors, introduced in $B(\omega)$ or $|\tau(\omega)|^2$ by an uncorrect form of the function $\omega_0 = \omega_0(a/g)$, are only small. A more accurate determination of this function would require more accurate measurements at a larger number of grids.
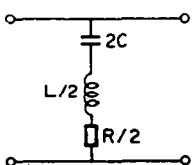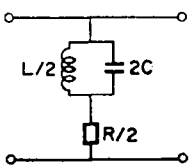
From the adaption of the various $|\tau(\omega)|^2$ curves it is guessed that for $a/g < 0 \cdot 2$ and $\omega < 0 \cdot 8$ the 2-element circuit represents $|\tau|^2$, $|\Gamma|^2$, $\sin^2 \psi_\tau$ and $\sin^2 \psi_\Gamma$ of thin *capacitive* grids correctly within less than 5 %, if Z_0 and ω_0 are taken from Fig. 9 and equation (14),

D

respectively. The grids may be considered as thin at least up to $t/g = 0\cdot02$. For thin *inductive* grids the same relations should be valid with the exception, however, that the limit is lower up to which an inductive grid may be treated as "thin".

In the Table 3 an ohmic resistor R has been included in the equivalent circuit to take account of the absorption of the grids. If R is placed at the indicated positions in the circuits, the resulting absorptivities become proportional to the reflectivities $|\Gamma|^2$, in accordance with the estimation (7). The value of this loss resistance follows from a comparison of (7) with A in Table 3:

$$R = (c/\lambda\sigma)^{\frac{1}{2}} \cdot \eta/2 \tag{15}$$

TABLE 3. IMPROVED EQUIVALENT CIRCUITS FOR THIN GRIDS*

Type of grid		Capacitive	Inductive
Equivalent circuit			
Resonant frequency		ω_o	
Normalized impedance of L and C at resonance		$Z_0 = \omega_o L = 1/\omega_o C$	
Generalized frequency		$\Omega = \omega/\omega_o - \omega_o/\omega = \lambda_o/\lambda - \lambda/\lambda_o$	
Normalized admittance	$Y(\omega) =$	$1/(R + jZ_o\Omega)$	$1/(R - - jZ_o/\Omega)$
Reflectivity	$\|\Gamma\|^2 =$	$\dfrac{1}{(1 + R)^2 + Z_o^2\Omega^2}$	$\dfrac{1}{(1 + R)^2 + Z_o^2/\Omega^2}$
	$\psi_\Gamma =$	$\pi - \arctan \dfrac{Z_o\Omega}{1 + R}$	$\pi + \arctan \dfrac{Z_o}{\Omega(1 + R)}$
Transmissivity	$\|\tau\|^2 =$	$\dfrac{R^2 + Z^2\Omega^2}{(1 + R)^2 + Z_o^2\Omega^2}$	$\dfrac{R^2 + Z_o^2/\Omega^2}{(1 + R)^2 + Z_o^2/\Omega^2}$
	ψ_τ	$\arctan \dfrac{Z_o\Omega}{R(1 + R) + Z_o^2\Omega^2}$	$- \arctan \dfrac{Z_o/\Omega}{R(1 + R) + Z_o^2/\Omega^2}$
Absorptivity	$A =$	$2R/\Gamma/^2$	

For complementary lossless grids: $C_{cap} = L_{ind}$ and $L_{cap} = C_{ind}$

* Resonance at $\omega = \omega_o$ and the losses are taken into account. Numerical values of Z_o and ω_o can be taken from Fig. 9 and equations (13), (14). $\lambda_o = g/\omega$ is the wavelength corresponding to ω_o

Because of the exponent $\frac{1}{2}$, R is only slightly dependent on frequency. The consideration of R is important mainly at the interference maxima of composed filters. There it reduces the peak transmission of the filters. It was mentioned that just from this reduction the absorptivity had been determined experimentally. Some values of R are given in Table 1.

With the introduction of the equivalent circuit it is possible now to describe the optical properties of a grid merely by the set of numbers Z_0, ω_0, and if neccessary, R. The first use of this representation will be made in the next section for the calculation of interference filters. The agreement of the calculated and the measured values in the quoted examples may be considered as an additional proof for the applicability of this representation and for the correct choice of the circuit parameters.

5. INTERFERENCE FILTERS WITH CAPACITIVE AND INDUCTIVE GRIDS

The far-infrared interference filter consisting of two inductive grids has already been the subject of some investigations.[1-4] New possibilities for filters with special properties are offered by the use of capacitive grids alone or in combination with inductive grids as reflectors. The most striking difference of purely "capacitive" filters to the older "inductive" filters is that now the interference orders do not lie harmonically in the frequency scale, as they almost do in the inductive filters. Also the finesse[5] is now *increasing* with frequency, in contrast to the inductive filters. For filters of the mixed type a wavelength dependence of the peak transmission exists due to the asymmetry of this filter.

The general equivalent circuit of an interference filter consisting of two grids is shown in Fig. 7(b). The methods of calculating the optical properties of the filter from this circuit and from the equivalent circuits of the grids (Table 2 or 3) are the subject of transmission line theory and need not be discussed here. One fact should be mentioned however: by the use of Fig. 7(b) one tacitly assumes the distance d of the grids to be large enough to insure that the interaction of the higher order diffraction modes of the grids may be neglected. The last of the examples of this section indicates that this interaction really is weak, even at rather small distances. Its influence on the transmissivity of the filter is estimated to be negligible if $d > g/3$.

5.1 *Symmetrical Filters*

An interference filter consisting of two identical, lossless, grids of susceptance $B(\omega)$ has its maxima of transmissivity at the frequencies ω_m following from

$$\cot (2\pi\omega_m d/g) - B(\omega) = 0 \tag{16}$$

Here $m = 1, 2, 3 \ldots$ is the order of interference. For thin inductive grids at low frequencies (Table 2) one has $B \approx 1/\omega L = \omega_0/\omega Z_0$, and (16) yields in good approximation

$$\omega_m = \frac{m}{2d/g - Z_0/\pi\omega_0} \tag{17}$$

These interference maxima lie harmonically. The reason is that the reflection phase ψ_r varies linearly with frequency if $\omega \ll 1$. If this interference filter is used as the dispersing element in a spectrometer, the harmonic distribution of the ω_m poses the same problems of overlapping orders and of necessary prefiltering as in a grating spectrometer. This difficulty may be overcome by the use of a filter of two capacitive grids: At low frequencies

(Table 2) one has B $\approx \omega C = \omega/\omega_0 Z_0$, and from (16) a non-harmonic distribution of the interference maxima follows:

$$\omega_m = \frac{m - \frac{1}{2}}{2d/g + 1/\pi\omega_0 Z_0} \tag{18}$$

At these low frequencies, the reflectivity $|\Gamma|^2$ of the capacitive grids is low, however, and the resulting finesse [5] of the filter would be too low for the filter to be useful. At higher frequencies, where the reflectivity is high enough to yield a sufficiently high finesse, the distribution of the ω_m is a more complex function of m than (18), but it still shows a pronounced deviation from the harmonic distribution. Hence an interference filter of two capacitive grids could be useful as prefilter in a far infrared monochromator of the grating type or of the type using an inductive interference filter.

As an illustration in Fig. 10 the measured transmissivity of an interference filter is shown consisting of two grid No. 1 on the support Fig. 5. The full line is the filter transmissivity calculated for the inserted equivalent circuit, using the parameters Z_0, ω_0, and R from Table 1. The distribution of the interference orders is non-harmonic. The
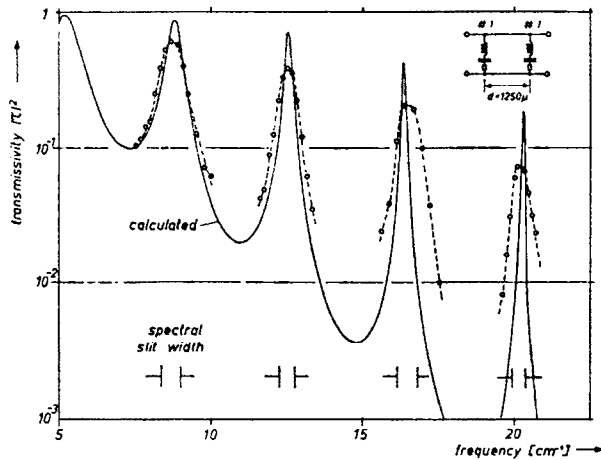

FIG. 10. The transmissivity of an interference filter consisting of two capacitive grids No. 1. The interference orders lie non-harmonically. The finesse increases with frequency, in contrast to filters of inductive grids. Distance of the grids $d = 1250\,\mu$.

widths of the interference maxima decreases with increasing frequency. The simultaneous decrease of the peak transmission is not only due to absorption in the grids, but also to imperfections of the grids, to deviations from their ideal parallelism and to the finite resolution of the spectrometer. The loss resistance R of the grids No. 1 (see Table 1) was chosen so that the calculated curve in Fig. 10 exceeds the measured curves by a reasonable amount. Therefore, this value of R includes influences of imperfections and poor parallelism besides the pure absorptivity.

5.2 Asymmetrical Filters

One stringent condition for an interference filter to show interference maxima with a peak transmission near unity is its optical symmetry, i.e.

$$Y_1(\bar{\nu}) = Y_2(\bar{\nu}) \tag{19}$$

must hold in an interference maximum at absolute* frequency $\bar{\nu}$. Filters made from two identical grids automatically possess this symmetry at all frequencies. A filter consisting of one inductive and one capacitive grid, however, can fulfil the condition (19) at only one frequency $\bar{\nu}$. Because of (9) both grids show equal transmissivities at $\bar{\nu}$, i.e. $\bar{\nu}$ is the frequency of the crossing point of the $|\tau|^2$ curves of both grids. If the distance d between the grids is chosen so that the resonance (16) is also satisfied at $\bar{\nu}$, the filter will have only this one interference maximum at $\bar{\nu}$ with nearly unit peak transmission. In the other interference maxima the peak transmission is reduced more or less due to the asymmetry of the filter. In a first approximation the variation of $|\tau|^2$ of the grids within the interference maxima may be neglected. Then the peak transmission of the filter in an interference maximum at frequency ν_m becomes [10]

$$|\tau(\nu_m)|^2 = \frac{|\tau_i(\nu_m)|^2 . |\tau_c(\nu_m)|^2}{[1 - |\Gamma_i(\nu_m)| . |\Gamma_c(\nu_m)|]^2} \tag{20}$$

This expression decreases with increasing asymmetry of the filter. This type of reduction of the peak transmission occurs even when the grids are perfectly conducting, ideally parallel and free of imperfections.

As an example a filter (see Fig. 11) has been combined from the grids No. 2 and No. 3. Their transmissivities are equal at $\bar{\nu} = 15$ cm^{-1}. The distance $d = 386\,\mu$ was chosen bringing the first order interference maximum ν_1 near $\bar{\nu}$. The full line in Fig. 11 is
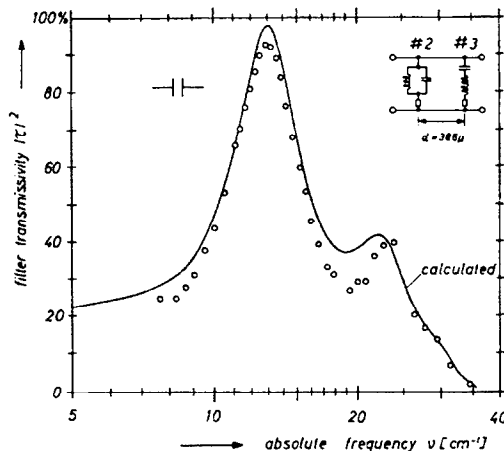

FIG. 11. The transmissivity of an interference filter combined from one inductive (No. 2) and one capacitive grid (No. 3). Distance of the grids $d = 386\,\mu$. The higher order interference maxima have low peak transmission because of the asymmetry of the filter.

again the theoretical transmissivity of the filter, calculated with the inserted equivalent circuit and the parameters from Table 1. The measured points agree satisfyingly with this curve. The first order interference maximum is found at $\nu_1 = 14 \cdot 2$ cm^{-1} and has $|\tau|^2_{max} = 92\%$. The second order maximum at $\nu_2 = 23$ cm^{-1} lies apparently non-harmonic, its peak transmission is only 40%, and the third order maximum is only weakly visible at 30 cm^{-1}.

* For the calculation of filters which consist of different grids it is necessary to use the absolute frequency ν rather than ω which was normalized specifically to each grid. If ν is measured in [cm^{-1}] one has $\omega = g.\nu$ for each grid.

The last of the examples follows from the preceeding if there the distance between the two grids is reduced as far as possible. The case $d = 0$ cannot be realized, however, because of the finite thickness of the grid, and also since unavoidable dust particles prevent a direct contact. Figure 12 shows the measured transmissivity of this device. The full line was calculated from the equivalent circuit of Fig. 11, but using the estimated distance $d = 30\,\mu$ of the grids. The general shape of this curve may be understood best for the limiting case $d = 0$. The equivalent circuit then contains the admittances of both grids connected in parallel (Fig. 12), i.e. it becomes of the type Fig. 7(a) with $Y = Y_c + Y_i$. The series
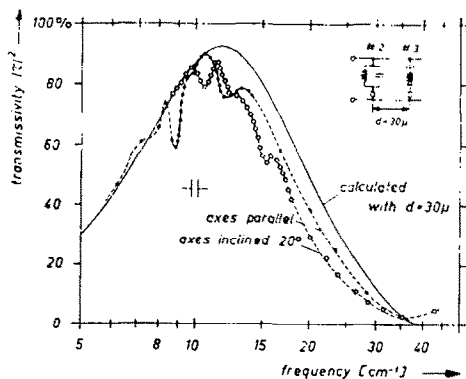

FIG. 12. Transmissivity of the filter of Fig. 11, but the distance of the grids now as low as possible. The interaction of the evanescent, higher order diffraction sidewaves causes the fine structure on the measured curves.

resonance ($Y \to \infty$) of the capacitive grid (L_c, C_c) near $\nu_c = 40\ \mathrm{cm}^{-1}$ is not affected by the presence of the inductive grid. This resonance causes the minimum of $|\tau|^2$ in Fig. 12. Below ν_c the admittance Y_c is capacitive, and it adds to the capacity C_i of the inductive grid. The parallel resonance (maximum of $|\tau|^2$) of the inductive grid is therefore shifted from the original resonant frequency $\nu_i = 27\ \mathrm{cm}^{-1}$ of the single inductive grid to a lower frequency $\nu = 11\ \mathrm{cm}^{-1}$ for the whole device. Below this new resonant frequency, this combination of two grids acts similarly to an inductive grid of $g = 900\,\mu$. In this calculation any interaction of the evanescent sidewaves of the grids has been neglected. The general agreement of the calculated curve with the measurements in Fig. 12 indicates that this interaction really is small, even at distances as low as $30\,\mu$. The magnitude of these interactions is recognized if one of the grids is rotated in its own plane so that it axes become inclined to the axes of the other grid (Fig. 12). The fine structure of the measured transmissivity changes rapidly even for a small rotation. This is interpreted to be caused by the dependence of the coupling of the higher order sidewaves on their directions of propagation. These are determined by the axes of the grids. The absolute changes in $|\tau|^2$ connected with a rotation are of the order of 10%. The reason for this low interaction may be the considerable difference in grid constants of the two grids, which determine the spatical periodicity of the sidewaves.

REFERENCES

1. RENK, K. F. and L. GENZEL, *Appl. Optics* 1, 643 (1962).
2. MITSUISHI, A., Y. OTSUKA, S. FUJITA, and H. YOSHINAGA, *Japan. J. appl. Phys.* 2, 574 (1963).
3. BELL, E. E., *Symposium on Molecular Structure and Spectroscopy* Columbus, Ohio (1962); P. VOGEL and L. GENZEL, *Infrared Phys.* 4, 257 (1964).
4. ULRICH, R., K. F. RENK and L. GENZEL, *IEEE Trans. on Microwave Theory and Technique*, Vol. MTT 11, 363 (1963).
5. BORN, M. and E. WOLF, *Principles of Optics*. Pergamon Press (1959).
6. MARCUVITZ, N., *Waveguide Handbook*. M.I.T. Rad. Lab. Ser., McGraw-Hill, (1951).
7. GENZEL, L. and R. WEBER, *Z. angew. Phys.* 10, 195 (1958).
8. RUSSEL E. E. and E. E. BELL, *Infrared Phys.* 6, 75 (1966).
9. SIMONYI, K., *Foundations of Electrical Engineering*. Pergamon Press (1963).
10. SMITH, S. D., *J. opt. Soc. Am.* 48, 43 (1958).

APPENDIX

The Preparation of the Capacitive Grids

The substrate of the capacitive grids must have low losses, i.e. it must be as thin as possible, and yet provide some mechanical strength to allow handling the grids and spanning them plainly. The thinnest available Mylar-film was 2·6 μ thick and was found usable in the low frequency region $\nu < 30$ cm^{-1} discussed above. At higher frequencies a thinner film would be preferable if low losses are desired. The mechanical strength of Mylar should be sufficient down to at least 1 μ thickness.

Before the preparation of the grids the Mylar film was baked a few hours at approximately 150°C to allow for some shrinkage in advance. The film then was glued on an annular frame (Fig. 5), was spanned over a thick, very slightly convex metal plate, and copper was vacuum-deposited on it (0·1 mg/cm^2). The copper layer was thickened to a few microns by galvanisation. A coating with light-sensitive laquer (Kodak Photo Resist KPR) was applied while the surface was spinning around a vertical axis. An inductive grid of the desired shape served as photographic negative. Usually wire-cloth was used, since here the thickness of the grids is of no importance. This grid was spanned, too, and pressed against the laquer. After exposition and development the unexposed copper areas were etched with FeCl$_3$ solution; rinsing and drying completed the preparation. The KPR coating should be sufficiently thin to reduce its contribution to the losses. It protects effectively the remaining metallic parts of the grids. By a variation of the etching time, grids within a certain range of a/g can be produced from the same original grid. For very long etching times, however, the metallic squares of the grid get rounded corners and become irregularly shaped. The grid No. 8 in Table 1 is an example for this case. It was originally identical with grid No. 1, but then it was etched again twice as long as before. Its transmissivity curve (see Fig. 3) cannot be fitted satisfyingly by a two-element equivalent circuit.